

## In situ self assembly of soft diclofenac loaded microparticles in superstructured fluids†

Cite this: *Soft Matter*, 2013, **9**, 10165

F. Benaouda,<sup>a</sup> Z. Bachoo,<sup>a</sup> M. B. Brown,<sup>bc</sup> G. P. Martin<sup>a</sup> and S. A. Jones<sup>\*a</sup>

This study investigated how the *in situ* construction and payload delivery from soft diclofenac loaded hydroxypropylmethylcellulose (HPMC) coated microparticles was influenced by the superstructure of the cosolvent in which the particles were suspended. A dual nozzle spray was used to produce microparticles in a propylene glycol (PG)-water mixture and data generated from the structural features of the vehicle, the physical properties of the particles and drug transport from the suspensions were used to characterise the particle-vehicle interactions. Infrared spectroscopy indicated supramolecular structures were formed in the bulk PG-water cosolvent upon mixing, but no solvent structural modification was observed as a consequence of microparticle self-assembly. Forming the microparticles in a premixed cosolvent, *i.e.*, with a preformed superstructure, did not allow the polymer to deposit on the surface of the microparticles. The suspensions that did not contain the HPMC coated microparticles demonstrated a reduced diclofenac transmembrane transport rate ( $7.9 \pm 0.4 \mu\text{g cm}^{-2} \text{ h}^{-1}$ ) compared to soft HPMC coated particles ( $27.7 \pm 3.0 \mu\text{g cm}^{-2} \text{ h}^{-1}$ ). The HPMC-diclofenac hydrogen bonding interactions observed in the polymer coated material, the increased availability of the diclofenac in the solution state (drug degree of saturation rose from  $3.0 \pm 0.2$  to  $11.0 \pm 1.2$ ) and the slower microparticle formation kinetics (>1 order of magnitude) supported the conclusion that the cosolvent supramolecular structuring controlled HPMC deposition at the particle interface. Analysis of the solid material recovered from the suspensions suggested that the cosolvent supramolecular structures could be used to modify the diclofenac solid-liquid equilibrium and generate a complex liquid with an unusually high chemical potential.

Received 1st July 2013

Accepted 6th September 2013

DOI: 10.1039/c3sm51796a

[www.rsc.org/softmatter](http://www.rsc.org/softmatter)

### Introduction

Soft matter structures can be engineered to respond to changes in both endogenous (*e.g.* pH, redox potential)<sup>1–4</sup> or exogenous stimuli (*e.g.* temperature, mechanical force).<sup>5–7</sup> This trait can be used to facilitate targeted administration of therapeutic agents. However, once a drug is released into a solution at a target site a sufficient concentration of the molecules must be allowed to accumulate to drive the function attributes assigned to therapeutically active molecules. For example, molecules often need to move across membranes or dock with receptor systems and if these processes occur passively a chemical potential gradient is required. The manner in which chemical potential gradients are created by the transient physical constructs formed during soft

matter fabrication, drug loading and release requires further investigation.

A number of different systems including those engineered to form microparticles,<sup>8–10</sup> hydrogels<sup>11,12</sup> and foams<sup>13–15</sup> have generated functional data to suggest that the chemical gradients created during drug delivery is a consequence of the release rate of the entity from the delivery assembly. These studies reflect the principles derived from the seminal theories proposed by Noyes and Whitney<sup>16</sup> and Higuchi<sup>17</sup> and have been supported by literature generated with a number of chemical species differing in physicochemical properties, *e.g.*, forskolin,<sup>10</sup> minoxidil<sup>14</sup> and vitamin E.<sup>15</sup> However, there are now some documented reports that suggest the relationship between the chemical potential and functional attributes of agents released from soft matter systems are more complex than first proposed.<sup>18,19</sup> A discourse has opened which suggests that the manner in which the carrier presents the delivered chemicals significantly influences their chemical potential. Ueda *et al.*,<sup>18</sup> have demonstrated that the co-localisation of liposomes with their released payloads at the surface of membranes altered the diffusion coefficient of the released species.<sup>18</sup> This was supported by measurements of hydrocortisone diffusion in the presence of cyclodextrin in the study described by Ribeiro *et al.*<sup>19</sup>

<sup>a</sup>King's College London, Institute of Pharmaceutical Science, Franklin-Wilkins Building, 150 Stamford Street, London, SE1 9NH, UK. E-mail: stuart.jones@kcl.ac.uk; Fax: +44 (0)207 848 4800; Tel: +44 (0)207 848 4843

<sup>b</sup>MedPharm Ltd., Unit 3/Chancellor Court, 50 Occam Road, Surrey Research Park, Guildford, GU2 Guildford, GU2 7AB, UK

<sup>c</sup>School of Pharmacy, University of Herts, College Lane Campus, Hatfield, Herts, AL10 9AB, UK

† Electronic supplementary information (ESI) available. See DOI: 10.1039/c3sm51796a



These phenomena could have an impact on a number of fields of research, but it is a particularly important consideration when high chemical potentials are needed to facilitate a particular function of the delivered chemical, for example, when agents are being driven across highly restrictive biological barriers.

The administration of therapeutic agents to the eye or the skin are just two examples of where the soft matter systems must generate a large chemical potential gradient in order to function effectively.<sup>2,14</sup> In such systems the relationship between chemical potential and release from the carrier is often complicated by both the supramolecular structures formed in the solvent and the interfacial phenomena that follow drug exit from the carrier. However, the magnitude and hence the significance of these effects remain unclear. The goal of the current study was to investigate the dynamic drug–vehicle interactions that occur during payload release from self-assembling soft matter systems. In particular, the aim was to investigate the role of macromolecules in the self-assembly process and gain a better understanding of how the carrier assembly influenced the chemical potential of the drug, when used in a system designed to promote the passage of a drug molecule through a hydrophobic barrier. In order to achieve this, soft hydroxypropylmethylcellulose (HPMC) microparticles in a superstructured PG–water cosolvent was employed as a model system. Infrared spectroscopy was used to analyse the cosolvent as this allowed C–H stretches of the PG alkyl groups to be recorded. Diclofenac, a pharmaceutically relevant solute, was utilised in this study in its unionised form as its behaviour within superstructured PG–water vehicles has been elucidated previously<sup>20</sup> and HPMC was employed as the polymer since it is known to have the capacity to form hydrogen bonds and control the process of soft matter self assembly.<sup>21,22</sup> As the system under investigation was dynamic, *i.e.*, it formed the drug carrier structures during the application of the system to a membrane, the drug saturation in the system could not be determined by simply assaying the drug solubility, thus a method that derived drug saturation from transport measurements was employed.

## Results

### Solvent structuring

The asymmetric C–H stretches of the alkyl groups observed at 2972, 2932 and 2878 cm<sup>−1</sup> in the pure PG solvent shifted to higher wavenumbers when a 0.3 volume fraction (*f*) of water was added to PG (Fig. 1a, peak assignment referenced to ref. 23–25). These shifts in the infrared spectra indicated CH···H interactions occurred within the cosolvent mixture.<sup>20,26–28</sup> The movement of the PG bands in the range 1400–1290 cm<sup>−1</sup>, assigned to the OH deformation vibration (Fig. 1a, peak assignment referenced to ref. 23 and 24), to higher frequencies when the water was added supported the conclusion that significant PG–water H-bonding occurred in the cosolvent. The bending vibration band of water (D<sub>2</sub>O) observed at 1219 cm<sup>−1</sup> for the 0.7 : 0.3 (v/v) PG–water mixture was 9 cm<sup>−1</sup> higher than that of the pure D<sub>2</sub>O solvent and this indicated water structuring was also weakened as a consequence of the introduction

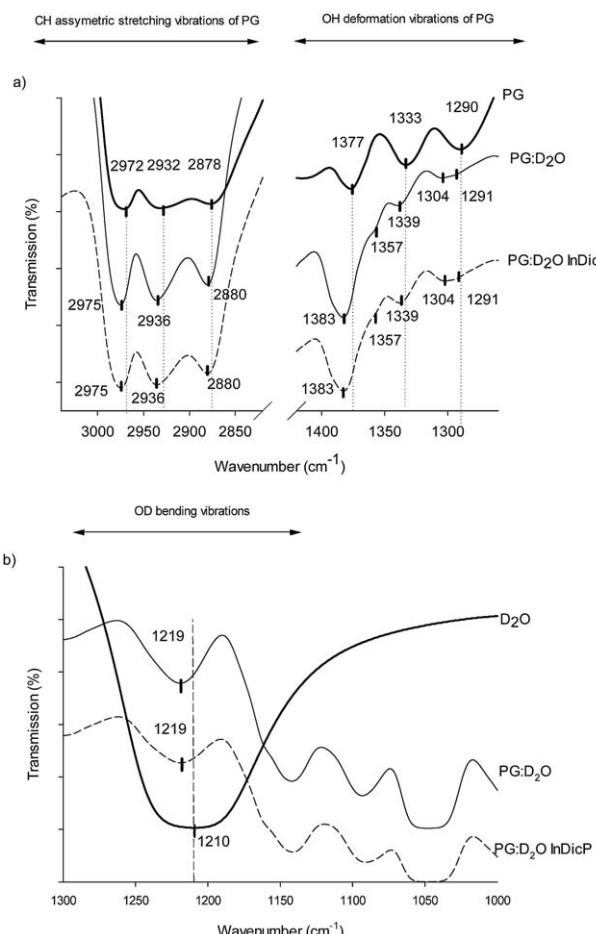


**Fig. 1** The solution state Fourier transform infrared spectra of propylene glycol (PG), water (deuterated D<sub>2</sub>O), a 70 : 30 (v/v) PG–D<sub>2</sub>O mixture and the self-assembled hydroxypropylmethylcellulose-coated microparticle in an equivalent PG–D<sub>2</sub>O vehicle (InDicP): (a) displays the CH asymmetric stretching (3200–2700 cm<sup>−1</sup>) and CH and OH deformation vibrations (1600–1150 cm<sup>−1</sup>) (b) displays the bending vibration of water (1300–1000 cm<sup>−1</sup>).

of PG into the vehicle (Fig. 1b). No additional spectral changes were induced by the addition of diclofenac or HPMC to the PG–water mixture (data not shown graphically) and the IR bands remained unaltered during the *in situ* self-assembly of the HPMC microparticles (InDicP, Fig. 1).

### Diclofenac solution state characteristics

Diclofenac (Dic) passed through the silicone membrane rapidly and no significant transport lag-time was observed when the permeation of the solubilised drug from the five calibration solutions was assessed (SS<sub>1</sub>–SS<sub>5</sub>). The steady-state flux was measured within the first 6 h of the Dic permeation profile as neither donor phase dose depletion or receiver phase saturation was found to hinder diffusion in this time period ( $R^2 > 0.99$ ) (ESI SI1a†). A linear relationship between DS and transport rate ( $R^2 = 0.98$ , ESI SI2†) was generated using the calibration solutions and this indicated that the transport conditions were well controlled across the series of experiments. The direct correlation between the theoretical DS, calculated by solubility

measurements (according to a method reported previously<sup>29</sup>), and the silicone transport results established the ability of the Franz cell test system to measure changes in drug saturation (DS) of the test solutions (gradient = 0.99,  $R^2 = 0.98$ , ESI SI1b†). The *in situ* self-assembled microparticles (InDicP) generated a 3.5-fold increase in the flux ( $27.7 \pm 3.0 \mu\text{g cm}^{-2} \text{ h}^{-1}$ ) compared to the equivalent suspension formed in a premixed cosolvent (DicP,  $7.9 \pm 0.4 \mu\text{g cm}^{-2} \text{ h}^{-1}$ ) (Fig. 2). Using the calibration curve, the DS in the application vehicle for InDicP during steady-state was calculated to be  $11.2 \pm 1.6$ . After 6 h steady-state flux was discontinued and at 30 h the DS was  $5.9 \pm 0.7$  in the microparticle suspension (ESI SI3†). The DicP test system displayed a DS of  $3.1 \pm 0.4$  during steady-state flux.

**Diclofenac solid state characteristics.** Recrystallising the drug in the presence of HPMC in the PG–water cosolvent produced a different crystal habit compared to the original diclofenac sourced from the supplier and the material recrystallised in the absence of the polymer. The *in situ* self-assembled diclofenac microparticles (InDicP) displayed a spherical morphology whereas in the absence of HPMC a star-shape morphology was observed (Fig. 3). The birefringence of the materials when exposed to cross polarised light indicated that the InDicP particles were crystalline in nature with the majority of crystalline material residing in the particle core (Fig. 4). The rate of InDicP microparticle production was linear between 5 and 60 min ( $R^2 = 0.97$ ,  $n = 3$ ), but after 60 min a state of

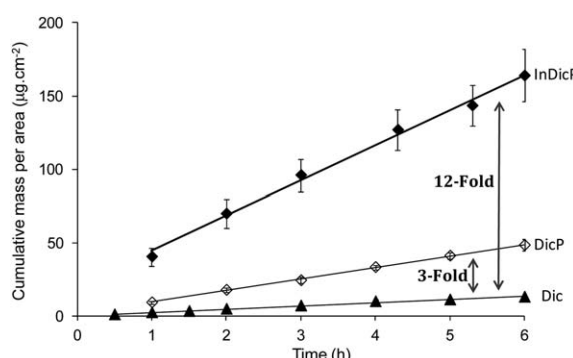


**Fig. 2** The transmembrane transport rate of diclofenac when the drug was presented as a saturated solution ( $\blacktriangle$ , Dic), as a microparticle suspension formed in a premixed propylene glycol (PG)–water vehicle ( $\diamond$ , DicP) and as the self-assembled hydroxypropylmethylcellulose-coated microparticle suspension ( $\blacklozenge$ , InDicP) ( $n = 5 \pm \text{SD}$ ).

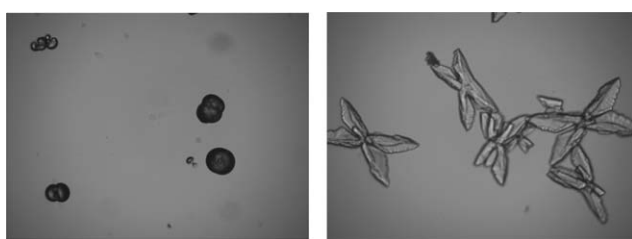


**Fig. 3** The light microscopy images of the diclofenac microparticles at a magnification of  $\times 200$ , left, recrystallised with hydroxypropylmethylcellulose (HPMC); right, recrystallised in the absence of HPMC.

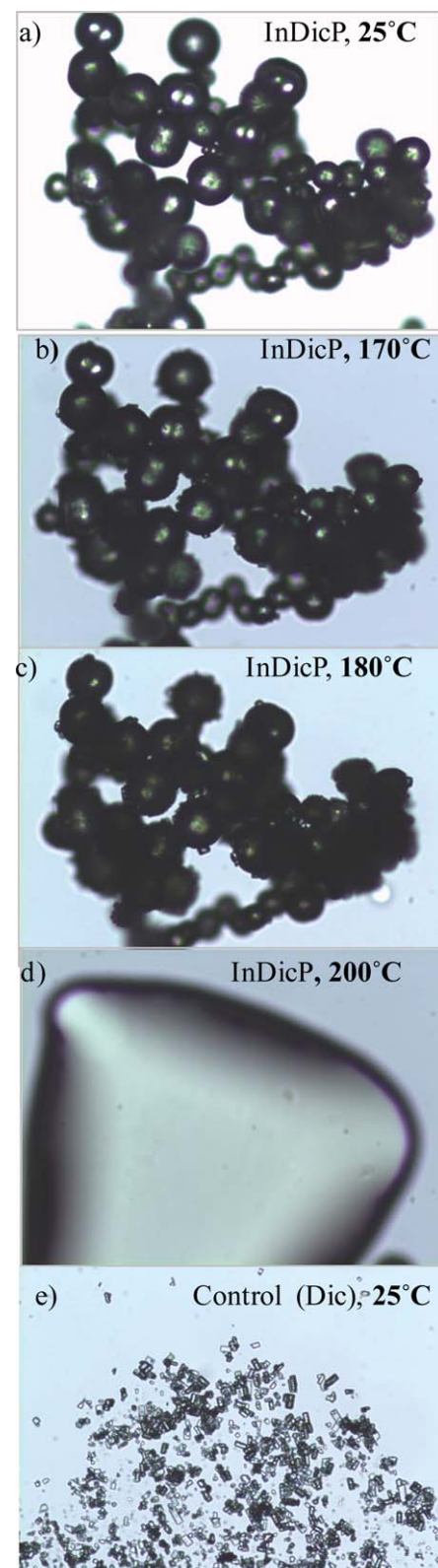


**Fig. 4** The morphology of the recovered crystals from the self-assembled hydroxypropylmethylcellulose (HPMC)-coated microparticle suspension (InDicP) at: (a)  $25^\circ\text{C}$ , (b)  $170^\circ\text{C}$ , (c)  $180^\circ\text{C}$  and (d)  $200^\circ\text{C}$  compared to those obtained from (e) the control suspension (Dic, recrystallised in the absence of HPMC) at  $25^\circ\text{C}$  at a magnitude of  $\times 200$ .



equilibrium between the solid and the solution phases was attained (Fig. 5). In the absence of HPMC, the linear phase of diclofenac re-crystallisation ( $1-30$  min,  $R^2 = 0.98$ ,  $n = 3$ ) was 18-fold faster and the solid-solution phase equilibrium was established 30 min prior to that observed for the InDicP system (Fig. 5). The microcrystals recovered from the InDicP system showed a reduction in their birefringence when heated to  $170$  °C (without the polymer this process was induced at  $180$  °C), which indicated that the material had started to melt (Fig. 4b and c). At  $200$  °C a molten liquid was observed for all samples (Fig. 4d). DSC analysis suggested that the product from the self assembly process did not solely consist of pure diclofenac as a second endothermic peak at  $88.6 \pm 0.4$  °C was observed in addition to the melting endothermic peak of diclofenac at  $173.3 \pm 1.8$  °C (Fig. 6a). The 30% w/w weight loss during the first of the two thermal transitions suggested that the recrystallised material contained a volatile component. Heating the samples beyond  $200$  °C produced a rapid decrease in the weight, which was attributed to sample decomposition (Fig. 6a). When the diclofenac crystals were formed in the absence of HPMC the two endothermic events shifted to  $95.3 \pm 8$  °C and  $177.1 \pm 0.5$  °C as a consequence of there being no drug–polymer interactions (Fig. 6b). The melting point of diclofenac acid was recorded using the same analysis methodology at  $179 \pm 0.5$  °C (ESI SI4†).

**Diclofenac release.** The release of the chemical payload from the microparticles was tested by assessing the ability of the system to saturate a vehicle after manufacture. Both InDicP and the control saturated a PG–water cosolvent within 2 h of their suspension in the cosolvent mixture. The saturated solubility of the InDicP compared to the control diclofenac material, recrystallised without HPMC, was 2-fold higher (at  $2.6 \pm 0.0$  mg mL $^{-1}$  vs.  $1.3 \pm 0.0$  mg mL $^{-1}$  at 24 h), which suggested the drug released from the two microparticulate systems were presented to the solvent in different physical forms. Monitoring the C=O stretching vibration of diclofenac using the FTIR measurement (Fig. 7), indicated that the diclofenac in the microparticles formed hydrogen bonds with HPMC (indicated by broadening of the band at  $1692$ – $1644$  cm $^{-1}$ ) and it was these bonds that

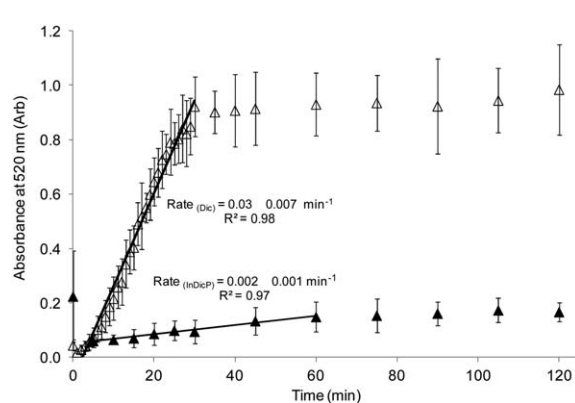


**Fig. 5** The rate of diclofenac re-crystallisation for a control system ( $\Delta$ , Dic, in the absence of hydroxypropylmethylcellulose (HPMC)) and the self-assembled HPMC-coated microparticle system ( $\blacktriangle$ , InDicP) ( $n = 3 \pm$  SD).

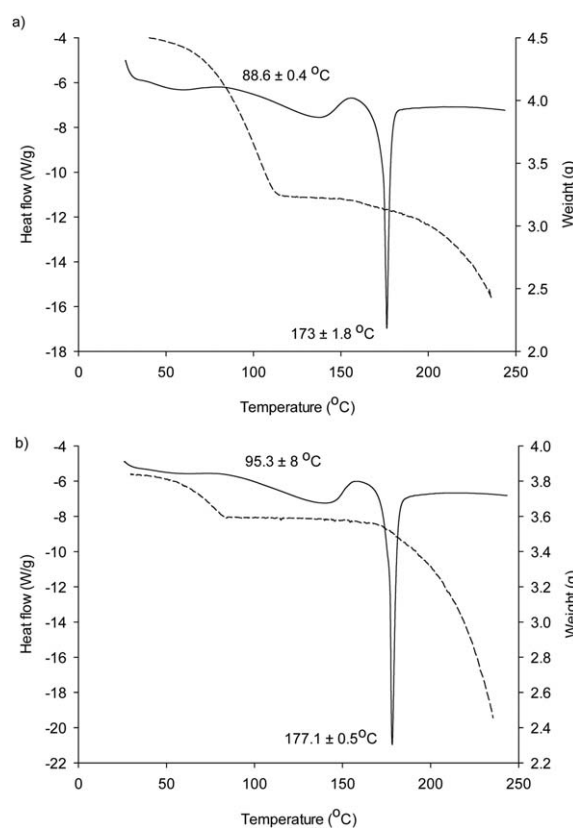


**Fig. 6** Differential scanning calorimetry (continuous line) and thermogravimetric scans (dotted line) of the solid material recovered from (a) the self-assembled hydroxypropylmethylcellulose (HPMC)-coated microparticle suspension (InDicP) and (b) the control suspension (Dic, recrystallised in the absence of HPMC).

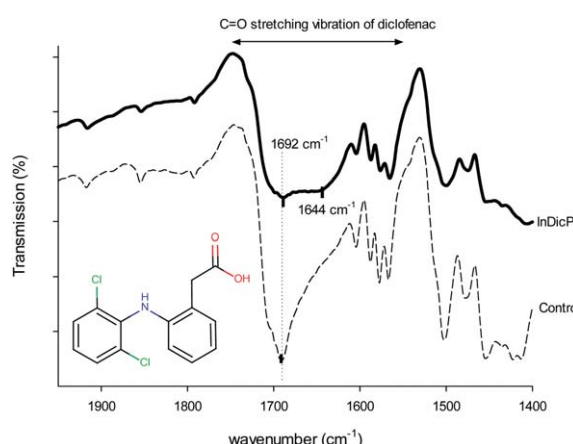


**Fig. 7** The Fourier transform infrared spectra of the recovered microparticles from the self-assembled hydroxypropylmethylcellulose (HPMC)-coated microparticle suspension (InDicP) (continuous line) and the control system (Dic, recrystallised in the absence of HPMC) (dotted line). The carbonyl stretching region ( $1950$ – $1400$  cm $^{-1}$ ) is shown.

appeared to hold diclofenac in a different conformation compared to both the diclofenac acid (C=O at  $1695$  cm $^{-1}$ , see ESI SI5†) and the diclofenac recrystallised from the same solvent system in the absence of the polymer (Fig. 7).



## Discussion

The FTIR analysis of the PG–water cosolvent mixture employed to form the HPMC coated soft microparticles confirmed the presence of the PG-rich supramolecular structures reported in previous work.<sup>23</sup> The *in situ* assembly of the microparticles did not modify the FTIR spectra, which suggested that the presence of the soft matter did not have a major impact on the supramolecular structure characteristics in the bulk solution (diclofenac at 20 mM and HPMC at 0.9% w/w).

Despite HPMC–drug hydrogen bond interactions having been previously identified with a number of solutes including diclofenac,<sup>30–34</sup> these interactions could not be observed directly in the liquid cell infrared spectra collected in this study. The sensitivity of infrared spectroscopy in the liquid state is limited by the large solvent signals recorded by the instrument, but previous work has shown that strong diclofenac–vehicle interactions can be detected using this method.<sup>35</sup> This suggests that if HPMC–drug interactions were present, they were relatively weak or localised to a particular area of the system. This conclusion is supported by the fact that a similar PG–water cosolvent mixture has been previously found not to hinder the diffusion of the solubilised diclofenac in the absence of a second solid phase,<sup>20</sup> and suggests that any solution state interactions between the drug and solvent supramolecular structure have a minimal functional effect in the bulk solution. Pygall *et al.*,<sup>33</sup> also showed that solution state interactions in the bulk solution (diclofenac concentration  $\leq$  60 mM, HPMC concentration  $1 \leq$  w/w%) did not affect diclofenac sodium self-diffusion when co-solubilised in aqueous solutions<sup>33</sup> and this was supported in the current work by the fact that diclofenac transmembrane transport using the system's calibration solutions followed ideal behaviour according to the Higuchi relationship.<sup>17</sup>

The recrystallisation, thermal analysis and solid-state FTIR data demonstrated that the presence of a second phase in the superstructured cosolvent, in the form of the soft matter, did influence the functional behaviour of diclofenac. However, the fact that the recrystallisation process only resulted in HPMC coated microparticles when the solvent superstructures were formed simultaneously in the vehicle, as shown by the microscopy images, suggested HPMC–diclofenac–solvent interactions were localised towards the interfacial regions of the microparticles. Incorporation of the diclofenac in the HPMC coated microparticles resulted in a higher chemical potential gradient in the solvent in comparison to when the drug was suspended in the solvent as uncoated crystals and this suggested that interfacial phenomena has a consequential effect on the manner that diclofenac behaved in the bulk solution. It is known that diclofenac can generate high chemical potential gradients upon *in situ* cosolvent mixing in systems that are metastable, but drug recrystallisation is traditionally thought to have deleterious effects on the high thermodynamic drug activities that result from this process due to drug loss from the bulk solution.<sup>36–38</sup> The unusual behaviour of the self-assembling soft matter system was attributed to modifications of the solid–liquid equilibrium during microparticle formation. In the bulk

solution of all of the systems the PG-rich supramolecular arrangements with water were shown by FTIR to assemble rapidly upon cosolvent mixing of PG. During this process the diclofenac molecules, which are known to be preferably held within the PG supramolecular structures by weak interactions, should remain in such structures (an image has been presented previously<sup>20</sup>) and not readily diffuse into the water clusters, until the high levels of drug supersaturation in the bulk solution overcome this restrictive environment to initiate the formation of a second phase in the solution. In the case of the system that generated the HPMC coated microparticles, the cosolvent appeared to interact with the polymer in a manner that it promoted the deposition of the latter at the surface of the drug crystals during formation of the second phase. This interface, when exposed to the bulk solution, appeared to have a distinctive effect on the diclofenac remaining in solution. The result of this was that drug self-association was reduced in a manner that retarded nucleation and provided a matrix to sustain the heightened levels of drug supersaturation compared to the drug crystal interface left uncoated by the polymer.<sup>39,40</sup> The ability of HPMC to increase the upper limit of drug saturation has been previously documented for single phase solutions, for example, oestradiol recorded a DS 13 for 6 h<sup>37</sup> and hydrocortisone a DS 4.8 for 6 h,<sup>41</sup> but such interfacial effects from *in situ* recrystallised material do not appear in this or similar studies regarding drug supersaturation.<sup>36–41</sup> This may be due to the fact that it is not common practice, when considering drug loaded soft matter systems, to analyse the bulk solution superstructuring and hence the prior data was not considered from the same perspective as the current work. It appears essential to consider the vehicle superstructure in the system presented in the current study as without an understanding of this higher level structuring in vehicle it would be problematic to explain the behaviour HPMC.

The approaches previously described in the literature that attempt to generate drug loaded vehicles with high chemical potentials put forward the perspective that crystal formation must be avoided as this would return the drug chemical potential of the vehicle to unity.<sup>39,41</sup> This is a logical conclusion if the high chemical potential is a property that the solution must display for an extended period of time (>days) as most drug supersaturated systems will show chemical potential depletion over time.<sup>41–43</sup> However, during the *in situ* soft microparticle production method employed in the current study, the simultaneous solvent supramolecular arrangement in the bulk solution appeared to generate a support system that used the drug crystallisation to enhance the heightened chemical potential of the cosolvent after mixing. This system was generated from a physically stable solution and produced a increased chemical potential for approximately one day, which is suitable for a wide range of pharmaceutical applications. It was interesting to note that the obtained DS of diclofenac in the solution state (DS *ca.* 12) was significantly higher than the maximum theoretical DS achievable in such a cosolvent system, determined at DS 7, when calculated using the drug solubilisation method.<sup>33</sup> Consequentially, the presence of the solid phase not only sustained the drug supersaturation in the bulk



solution for an extended period of time compared to a single phase system, in a similar manner to the work by Ueda *et al.*,<sup>18</sup> but it also increased the maximum thermodynamic activity the drug could attain in the solution. The drug solubilisation method records the DS upon the establishment of solid–liquid equilibrium and hence the difference in the maximum DS for the HPMC coated suspension systems was probably a consequence of the temporal dynamics of the solvent mixing upon the actuation of the dual sprays. The formation of the micro-crystals most probably generates a reservoir for subsequent membrane transport during the 30 h period that acts to replenish diclofenac in the solution state, which could, depending on the kinetics of the process, contributed to the higher than anticipated level of DS in the bulk solution. The drug release data supported this hypothesis as the diclofenac solubilised in the solution state was influenced by the PG–water supramolecular structure in a manner which favoured the re-dissolution of the solid into the solution, but how this process functioned to specifically increase transport cannot be elucidated by the current data set and presents an interesting concept that could be studied in future work.

The solid state FTIR data which showed the broadening of the C=O stretching vibration toward lower wavenumbers (range 1692–1644 cm<sup>−1</sup>) suggests that HPMC–diclofenac hydrogen bonding restricted the COOH of Dic and OH of HPMC. Comparable shifts of C=O diclofenac stretching, from 1692 cm<sup>−1</sup> to 1644 cm<sup>−1</sup>, has been associated with molecular restriction incurred as a consequence of salt formation<sup>44</sup> (the data have been confirmed using the diethylamine salt in this work, ESI SI5†). The presence of an HPMC–diclofenac interaction in the solid-state again suggests that some solution state interactions were occurring that were unique to the soft HPMC coated microparticles. The control imposed by the HPMC on the rate of *in situ* re-crystallisation (18-fold reduction in the re-crystallisation rate) and the alteration of diclofenac crystal morphology supported the presence of specific HPMC–diclofenac interactions during the transition from the solution to the solid state form. It was evident from the particle images that the crystalline material was retained in the particle core and the amorphous HPMC primarily on the particle exterior but, the exact nature of the interface that diclofenac presented to the HPMC could not be resolved by the analytical techniques employed in this study. Since the HPMC coated microcrystals retained a significant proportion of their crystalline nature, it was evident that the Dic–HPMC interactions were not strong enough to completely overcome the drug–drug interactions, if this was the case, the polymer would embed the drug in an amorphous matrix as observed with other drug–polymer systems.<sup>45,46</sup> In the absence of HPMC, the rapid mixing of the solvents (PG and water) generated smaller imperfect crystals which are known to be a feature of rapid nucleation and crystallization kinetics.<sup>39</sup> In the presence of HPMC, if the nucleation was controlled by the polymer alone, larger more uniform crystals would have been expected,<sup>39</sup> but spherical objects which had a HPMC coating suggested that the supramolecular structured solvent also played a role in the crystal formation. The superior release of diclofenac from the InDicP microcrystals

was typical of drug polymorph formation and this would be in accordance with other compounds containing a carboxylic acid moiety.<sup>47–50</sup> A more detailed investigation would be required to elucidate the exact crystal arrangement of diclofenac obtained in the *in situ* self-assembled InDicP system, but this fell outside the scope of the current study which was primarily interested in the solution state properties.

## Conclusion

Assembling HPMC coated microparticles loaded with diclofenac, in a cosolvent that was simultaneously forming supramolecular structures, generated a suspension with a high chemical potential. The HPMC interacted with the diclofenac through hydrogen bonding and this resulted in the polymer being drawn to the solid–liquid interface during particle formation to encapsulate the drug. The kinetics of the self-assembly process for the materials used in this study favoured drug dissolution in a manner that supported sustained and enhanced diclofenac thermodynamic activity when the cosolvent superstructure assembled simultaneously with the microparticle generation. The heightened diclofenac thermodynamic activity resulted in superior transmembrane transport compared to suspensions that presented self-assembled microparticles without the simultaneous solvent supramolecular structure formation. The HPMC coated diclofenac microparticles employed in this study functioned to exemplify the manner in which cosolvent supramolecular structuring influenced soft matter assembly at the surface of hydrophobic barriers. It is anticipated that this can provide a basis to fabricate novel pharmaceutical materials capable of delivering chemical entities in a range of biomedical scenarios to environments where high chemical potentials are required to elicit a functional response.

## Experimental

### Materials

Diclofenac, as the diethylamine salt, (BP grade, 99.9%) was provided by Unique Chemicals, India. HPMC (Metolose, grade 65SH, viscosity 50Cp), was a gift from Shin-Etsu Chemical Ltd, Japan. Propylene glycol (PG) (≥99.5%) was supplied from Sigma Aldrich, UK. Acetonitrile and methanol (High Performance Liquid Chromatography (HPLC) grade) were obtained from Fisher Scientific International, UK. Ethanol (99.7–100%) was provided by BDH laboratory supplies, UK. Phosphate buffered saline (PBS, pH 7.2, 0.172 M) tablets were supplied by Oxoid Ltd, UK. Sheets of silicone membrane (Folioxane®), with a thickness of 120 µm, were purchased from Novatech Ltd, France. De-ionised water (electrical conductivity 0.5–1 µS) was used throughout this study.

### Test system preparation

The self-assembled InDicP microparticles were generated using a dual-pump spray (100 µL metered nozzle); diclofenac saturated PG was contained in one canister and HPMC (3% w/v) dissolved in water (PBS, 0.172 M, pH 3) in the second. The diclofenac-saturated PG solution was produced by adding



excess of diclofenac diethylamine salt (DDEA) to PG adjusting to pH  $3 \pm 0.1$  with phosphoric acid, continually stirring at  $25^\circ\text{C}$ , for 72 h ( $>48$  h was required to ensure equilibrium solubility was attained in PG, kinetic data recorded but not shown), centrifuging the suspension for 20 min at 16 060g (Biofuge pico, Heraeus, Kendro Laboratory Products plc, UK) and removing the supernatant from the saturated suspension. The final pH of the solutions was checked and recorded (pH  $3 \pm 0.1$ ). To form the InDicP microparticles the dual spray formulations were simultaneous actuated and allowed to mix in a manner that achieved a vehicle composition of 0.7 : 0.3 (v/v) PG–water containing 0.59% w/v diclofenac and 0.9% w/v HPMC. DicP, an equivalent suspension, was produced in a solvent that had been mixed prior to the addition of diclofenac (0.59% w/v). The diclofenac-transport calibration solutions (SS) were prepared in a 0.7 : 0.3 (v/v) PG–water binary vehicle using the methods outlined previously in Benaouda *et al.*<sup>20</sup> The drug load in the SS PG solution required to generate a particular DS was derived using eqn (1).

$$[\text{Dic}]_{\text{PG}} = [\text{Dic}]_{\text{eq.}} \times \text{DF} \times \text{DS} \quad (1)$$

where  $[\text{Dic}]_{\text{PG}}$  was the initial diclofenac concentration in PG (mg  $\text{mL}^{-1}$ ),  $[\text{Dic}]_{\text{eq.}}$  the saturated equilibrium solubility (mg  $\text{mL}^{-1}$ ) in the PG–water cosolvent solution, DF the dilution factor (in this case the DF was 1.43), and DS was the degree of saturation. Five calibration solutions with varying DS in the range of 1–5 were prepared solutions (SS<sub>1</sub>, SS<sub>2</sub>, SS<sub>3</sub>, SS<sub>4</sub> and SS<sub>5</sub>). The absence of crystals in the calibration solutions was confirmed visually using an optical microscope (Olympus BX50F, Japan) at magnification of 200 $\times$  by monitoring a 1 mL aliquot of each solution in a multiwell plate (Greiner® multiwell plates, Sigma Ltd., UK) for 36 h.

### Solvent–solvent interactions

The molecular interactions that occurred in the pure solvents and the binary PG–water solution, at 0.7 : 0.3 (v/v), were assessed using a demountable universal liquid transmission cell system (Omni-Cell, Specac Ltd., UK) fitted with CaF<sub>2</sub> windows and a 25  $\mu\text{m}$  mylar spacer (Specac Ltd., UK) with spectrum One Fourier transform infrared (FTIR) spectrometer (Perkin Elmer Ltd., UK). Deuterated water (D<sub>2</sub>O) was employed to construct the systems, which were each carefully controlled at pH  $3 \pm 0.1$ , to allow visualisation of PG absorption bands in the 1700–1300  $\text{cm}^{-1}$  range. The InDicP system was formed and the solvent analysed over a time course that spanned from 2 to 180 min. All spectra were produced using 32 scans collected at a spectral resolution of 4  $\text{cm}^{-1}$  using the Spectrum software (version 10, Perkin Elmer Ltd., UK).

**Diclofenac solution state characteristics.** The chemical potential of diclofenac was assumed to be reflected by the measured degree of saturation in the solution state and this was determined through the assessment of transmembrane transport. Individually calibrated upright Franz diffusion cells (MedPharm Ltd, UK) with a diffusional area of  $\sim 2.1 \text{ cm}^2$  and receptor volume of  $\sim 10.8 \text{ mL}$  were employed for the transport studies. Disks of silicone membrane (measured thickness of

124.17  $\mu\text{m} \pm 6.01$  ( $n = 54$ )) were fitted, and sealed between the two diffusion cell chambers. The receptor compartment was filled with a previously sonicated and filtered receiver phase consisting of 20 : 80 EtOH–PBS (pH 7.4). The assembled Franz cells were placed into a VarioMag® magnetic stirrer plate immersed in a water bath (Grant Instruments, UK) at  $29^\circ\text{C}$  to maintain the silicone membrane and the donor phase at  $25^\circ\text{C}$ . A total of 10 actuations from the dual spray formulation, which generated *ca.* 1 mL of InDicP system, was applied to the apical surface of the silicone membrane and the degree of drug saturation (DS) was determined by comparison to the transport of diclofenac from a series of pre-formed calibration solutions (SS<sub>1</sub>, SS<sub>2</sub>, SS<sub>3</sub>, SS<sub>4</sub> and SS<sub>5</sub>). Aliquots of the receiver fluid (1 mL) were removed periodically and replaced immediately with the same volume of fresh receiver fluid, in order to monitor the diclofenac membrane penetration. The removed samples were analysed immediately for diclofenac content by HPLC. All the transport experiments were repeated 5 times and all the data were used. The lag time ( $T_L$ ) was obtained by extrapolation of the steady-state gradient from each individual Franz cell experiment.

**Diclofenac solid state characteristics.** The rate of the *in situ* diclofenac microparticle self assembly was monitored using ultraviolet spectroscopy in the presence and absence of HPMC. The test systems were generated *in situ* in the measuring cuvette and were gently mixed by hand to homogenise the suspension prior to analysis. The non-specific absorption at 520 nm was monitored at appropriate intervals over 120 min time period. The morphology of the product in each suspension was investigated using an optical microscope (Olympus BX50F, Japan) at a magnification of 200 $\times$ . The solid was recovered 2 h after initiation of the self assembly process using a 0.2  $\mu\text{m}$  nylon filter (Whatman, UK). Thermomicroscopic analysis of the recovered material was performed on a FP 82 hot stage module (Mettler Toledo, UK) mounted on a Leica DME long distance objective microscope with or without cross polarizing filters (Leica Microsystems, Germany) and an FP 90 thermal controller module (Mettler-Toledo, UK). Samples were heated at a rate of  $10^\circ\text{C min}^{-1}$  from 30 to  $250^\circ\text{C}$ . Differential scanning calorimetry (DSC) (TA Instruments, UK) and thermogravimetric analysis (TGA) (TA Instruments, UK) analysis were performed on accurately weighed samples (3–5 mg) under nitrogen purge at a heating rate of  $10^\circ\text{C min}^{-1}$  up to  $250^\circ\text{C}$ . For DSC analysis, sealed aluminium pans, with a vent hole pierced in the lid, were used in both the reference (empty) and the sample (test) positions. DSC and TGA instruments were calibrated according to the manufacturer's instructions using an indium standard. The melting points were taken as the point of intersection between the extrapolated baseline before the onset of the endothermic event and the extrapolated down slope of the peak. All DSC experiments were carried out in triplicate. Fourier transform infrared spectroscopy analysis was performed using KBr disks on a Spectrum One spectrometer (Perkin Elmer Ltd., UK). All spectra were produced using 32 scans collected at a spectral resolution of 4  $\text{cm}^{-1}$ . Spectral analysis was performed with Spectrum software (version 10, Perkin Elmer Ltd., UK). The kinetic solubility profiles of the solid material recovered from



the suspensions were determined in 0.7 : 0.3 (v/v) PG–water solutions (pH 3). At pre-determined time intervals, 1 mL aliquots were removed from the suspensions maintained under constant stirring conditions, and the samples centrifuged for 20 min at 13 000 rpm (Biofuge pico, Kendro Laboratory Products plc, UK). The drug-saturated supernatant was diluted in PBS (pH 7.4) and assayed for drug content using ultraviolet (UV) spectroscopy (Varian Cary 50 Bio UV-visible spectrophotometer, Varian Inc., US) at 275 nm. The UV diclofenac calibration curve was linear ( $R^2 > 0.99$ ) within the range of 1 to 100  $\mu\text{g mL}^{-1}$  with no matrix interference, the assay limit of detection (LOD) was 1.4  $\mu\text{g mL}^{-1}$ .

### Diclofenac quantification

Quantitative determination of diclofenac in the transport studies was performed using a reverse phase HPLC system consisting of a Jasco UV detector and pump (Jasco Corporation Ltd, UK). The mobile phase comprised acetonitrile–methanol–formate buffer (25 mM) (50 : 20 : 30 (v/v), pH 3.5) set at a flow rate of 1.2  $\text{mL min}^{-1}$ . Diclofenac was eluted using a Gemini® C18 (250  $\times$  4.6 mm) stationary phase (Phenomenex, UK) at room temperature with a 20  $\mu\text{L}$  injection volume and UV detection at 275 nm. The retention time for diclofenac was 7.5 min. The calibration curves were constructed on the basis of the peak area measurements using standard solutions of known diclofenac concentrations dissolved in an identical fluid as the receiver phase for the permeation studies. The assay was previously shown to be ‘fit for purpose’.<sup>19</sup>

### Statistical analysis

All values were expressed as their mean  $\pm$  standard deviation (SD), and statistical analysis of data was performed using the statistical package for social sciences SPSS version 16.0 (SPSS Inc., Chicago, IL, USA). Normality (Sapiro-Wilk) and homogeneity of variances (Levene’s test) of the data was assessed prior to statistical analysis. Permeation results were analysed statistically using one way analysis of variance (ANOVA) tests with *post hoc* Tukey analysis where required. All other data were analysed using a Student’s *t*-test. Statistically significant differences were assumed when  $p \leq 0.05$ .

### Acknowledgements

We gratefully acknowledge the financial support (FB) from the Algerian Ministry of Higher Education and Scientific Research.

### References

- 1 M. H. Li and P. Keller, *Soft Matter*, 2009, **5**, 927–937.
- 2 M. A. C. Stuart, W. T. S. Huck, J. Genzer, M. Muller, C. Ober, M. Stamm, G. B. Sukhorukov, I. Szleifer, V. V. Tsukruk, M. Urban, F. Winnik, S. Zauscher, I. Luzinov and S. Minko, *Nat. Mater.*, 2010, **9**(2), 101–113.
- 3 E. G. Bellomo, M. D. Wyrsta, L. Pakstis, D. J. Pochan and T. J. Deming, *Nat. Mater.*, 2004, **3**(4), 224–248.
- 4 E. R. Gillies, T. B. Jonsson and J. M. J. Frechet, *J. Am. Chem. Soc.*, 2004, **126**, 11936–11943.
- 5 N. I. Abu-Lail, M. Kaholek, B. LaMattina, R. L. Clark and S. Zauscher, *Sens. Actuators, B*, 2006, **114**, 371–378.
- 6 D. Mertz, J. Hemmerle, J. Mutterer, S. Ollivier, J. C. Voegel, P. Schaaf and P. Lavalle, *Nano Lett.*, 2007, **7**(3), 657–662.
- 7 Y. F. Lu, H. Y. Fan, N. Doke, D. A. Loy, R. A. Assink, D. A. LaVan and C. J. Brinker, *J. Am. Chem. Soc.*, 2000, **122**, 5258–5261.
- 8 S. Das and P. K. Suresh, *J. Nanomed. Nanotechnol.*, 2011, **7**(2), 242–247.
- 9 S. P. Vyas, M. Kannan, S. Jain, V. Mishra and P. Singh, *Int. J. Pharm.*, 2004, **269**, 37–49.
- 10 S. Gupta, M. K. Samanta and A. M. Raichur, *AAPS PharmSciTech*, 2010, **11**(1), 322–335.
- 11 A. Rozier, C. Maznel, J. Grove and B. Plazonnet, *Int. J. Pharm.*, 1989, **57**, 163–168.
- 12 J. Carlfors, K. Edsman, R. Petersson and K. Jornving, *Eur. J. Pharm. Sci.*, 1998, **6**(2), 113–119.
- 13 L. Andreassi, A. Giannetti and M. Milani, *Br. J. Dermatol.*, 2003, **148**, 134–138.
- 14 J. Rundegren, A. Westin and B. Kohut, *J. Invest. Dermatol.*, 2005, **124**, A98.
- 15 Y. J. Zhao, M. Moddaresi, S. A. Jones and M. B. Brown, *Eur. J. Pharm. Biopharm.*, 2009, **72**, 521–528.
- 16 A. A. Noyes and W. R. Whitney, *J. Am. Chem. Soc.*, 1897, **19**(12), 930–934.
- 17 T. Higuchi, *J. Soc. Cosmet. Chem.*, 1960, **11**, 85–97.
- 18 K. Ueda, K. Higashi, W. Limwikrant, S. Sekine, T. Horie, K. Yamamoto and K. Moribe, *Mol. Pharm.*, 2012, **9**(11), 3023–3033.
- 19 A. C. F. Ribeiro, L. M. P. Verissimo, C. I. A. V. Santos, A. M. T. D. P. V. Cabral, F. J. B. Veiga and M. A. Esteso, *Int. J. Pharm.*, 2013, **441**(1–2), 352–355.
- 20 F. Benaouda, M. B. Brown, S. Ganguly, S. A. Jones and G. P. Martin, *Mol. Pharm.*, 2012, **9**, 2505–2512.
- 21 A. R. Patel, J. Ashok, J. Nijssse and K. P. Velikov, *Soft Matter*, 2011, **7**(9), 4294–4301.
- 22 N. Jongen, P. Bowen, J. Lemaitre, J. C. Valmalette and H. Hofmann, *J. Colloid Interface Sci.*, 2000, **226**, 189.
- 23 P. Buckley and P. Giguere, *Can. J. Chem.*, 1967, **45**, 397.
- 24 G. Socrates, *Infrared Characteristic Group Frequencies*, John Wiley & Sons, New York, 1994.
- 25 Y. Su, J. Wang and H. Liu, *J. Phys. Chem. B*, 2002, **106**, 11823–11828.
- 26 E. Cubero, M. Orozco, P. Hobza and F. Luque, *J. Phys. Chem. A*, 1999, **103**, 6394–6401.
- 27 M. Dangelo, G. Onori and A. Santucci, *J. Chem. Phys.*, 1994, **100**, 3107–3113.
- 28 Y. Gu, T. Kar and S. Scheiner, *J. Am. Chem. Soc.*, 1999, **121**, 9411–9422.
- 29 F. Benaouda, M. B. Brown, G. P. Martin and S. A. Jones, *Pharm. Res.*, 2012, **29**, 3434–3442.
- 30 T. Hino and J. L. Ford, *Int. J. Pharm.*, 2001, **226**, 53–60.
- 31 C. B. McCrystal, J. L. Ford and A. R. Rajabi-Siahboomi, *J. Pharm. Sci.*, 1999, **88**, 792–796.
- 32 C. B. McCrystal, J. L. Ford and A. R. Rajabi-Siahboomi, *J. Pharm. Sci.*, 1999, **88**, 797–801.



33 S. R. Pygall, P. C. Griffiths, B. Wolf, P. Timmins and C. D. Melia, *Int. J. Pharm.*, 2011, **405**, 55–62.

34 A. Ridell, H. Evertsson, S. Nilsson and L. O. Sundelof, *J. Pharm. Sci.*, 1999, **88**(11), 1175–1181.

35 F. Benaouda, M. B. Brown, B. Shah, G. P. Martin and S. A. Jones, *Int. J. Pharm.*, 2012, **439**, 334–341.

36 A. F. Davis and J. Hadgraft, *Int. J. Pharm.*, 1991, **76**, 1–8.

37 N. A. Megrab, A. C. Williams and B. W. Barry, *J. Controlled Release*, 1995, **36**, 277–294.

38 F. P. Schwab, G. Imanidis, E. W. Smith, J. M. Haigh and C. Surber, *Pharm. Res.*, 1999, **16**, 909–915.

39 A. S. Myerson and R. Ginde, in *Handbook of industrial crystallisation*, Butterworth Henemann, Boston, 1992, pp. 45–46.

40 S. L. Raghavan, A. Trividic, A. F. Davis and J. Hadgraft, *Int. J. Pharm.*, 2001, **212**, 213–221.

41 S. L. Raghavan, B. Kiepfer, A. F. Davis, S. G. Kazarian and J. Hadgraft, *Int. J. Pharm.*, 2001, **221**, 95–105.

42 M. L. Leichtnam, H. Rolland, P. Wuthrich and R. H. Guy, *J. Pharm. Sci.*, 2006, **95**, 1693–1702.

43 M. F. Coldman, B. J. Poulsen and T. Higuchi, *J. Pharm. Sci.*, 1969, **58**, 1098.

44 K. M. O'Connor and O. I. Corrigan, *Int. J. Pharm.*, 2001, **226**, 163–179.

45 E. J. Kim, M. K. Chun, J. S. Jang, I. H. Lee, K. R. Lee and H. K. Choi, *Eur. J. Pharm. Biopharm.*, 2006, **64**(2), 200–205.

46 H. Konno, T. Handa, D. E. Alonzo and L. S. Taylor, *Eur. J. Pharm. Biopharm.*, 2008, **70**(2), 493–499.

47 J. Haleblia and W. Mccrone, *J. Pharm. Sci.*, 1969, **58**, 911.

48 M. Pudipeddi and A. T. M. Serajuddin, *J. Pharm. Sci.*, 2005, **94**, 929–939.

49 N. Jaiboon, K. Yos-In, S. Ruangchaithaweesuk, N. Chaichit, R. Thutivoranath, Siritaedmukul and S. Hannongbua, *Anal. Sci.*, 2001, **17**, 1465–1466.

50 Ö. Almarsson and M. J. Zaworotko, *Chem. Commun.*, 2004, 1889–1896.

